



Research paper

Experimental investigation on mode II fracture performance of old-new concrete

Shuang Liu^{1,2}, Zhenwu Shi³, Tao Jiang⁴, Huili Wang⁵

Abstract: The old-new concrete interface is the weakest part in the composite structure, and there are a large number of microcracks on the interface. In order to study the mode II fracture performance of the bonding surface of old-new concrete, the effect of planting rebar and basalt fiber is investigated. Nine Z-shaped old-new concrete composite specimens with initial cracks are made. Nine shear fracture load-displacement curves are obtained, and the failure process and interface fracture are discussed. On this basis, the mode II fracture toughness and fracture energy are obtained. The regression equations for fracture toughness and fracture energy are deduced with analysis of variance (ANOVA). The results show that fracture toughness and fracture energy increase with the increase of planting rebar number and basalt fiber content. With the increase of the planting rebar number, mode II fracture toughness and fracture energy increase more significantly. Planting rebar is the major factor for mode II fracture performance.

Keywords: new-old concrete, planting rebar, basalt fiber, mode II fracture, fracture toughness, fracture energy

¹PhD., School of Civil Engineering, Northeast Forestry University, 150040 Harbin, China, e-mail: 120896328@qq.com, ORCID: 0000-0002-7971-4991

²Senior engineer, Heilongjiang Transportation Investment Engineering Construction CO., LTD, Heilongjiang Transportation Investment Group Co, 150040 Harbin, China, e-mail: 120896328@qq.com, ORCID: 0000-0002-7971-4991

³Prof., School of Civil Engineering, Northeast Forestry University, 150040 Harbin, China, e-mail: shizhenwu@126.com, ORCID: 0000-0002-0860-5923

⁴PhD., Senior engineer, National & Local Joint Engineering Laboratory of Bridge and Tunnel Technology, Dalian University of Technology, 116023 Dalian, China, e-mail: 308239466@qq.com, ORCID: 0000-0002-0116-6307

⁵Associate professor, National & Local Joint Engineering Laboratory of Bridge and Tunnel Technology, Dalian University of Technology, 116023 Dalian, China, e-mail: wanghuili@dlut.edu.cn, ORCID: 0000-0002-0675-2524

1. Introduction

Nowadays many concrete structures have entered the stage of reinforcement, maintenance and reconstruction. The expanded section method is a commonly used reinforcement method, which removes the old concrete and pours a layer of new concrete on the hard concrete aggregate [1–3]. However, the interfacial bond between old-new concrete is the key issue of expanded section method [4–6].

Scholars have done a lot of research work on the bonding performance of old-new concrete. He studied the effects of different treatment methods, interfacial agents and freeze-thaw cycles on the bonding properties of old-new concrete. It was found that the surface of old concrete should be roughened before bonding, and cement paste is the best interface agent [7]. Fan investigated the influence of old concrete age, interface roughness and freeze-thawing attack on new-to-old concrete structure [8]. Wang presented both theoretical and experimental studies of the long-term behavior of prestressed old-new concrete composite beams under sustained loads [9]. Cheng discussed the effect of planting rebar on the shear performance of the old-new concrete interface, and concluded that the failure mode of the old-new concrete interface was splitting shear failure [10]. Zhang designed Z-shaped specimen, studied the influence of different carbonization depth of old concrete surface, and found that concrete carbonization can enhance the interfacial bond strength [11]. Liang explored the direct shear state, fracture surface displacement, deformation and crack location of the new to old concrete bonding interface through the shear test of rectangular beam [12]. The above studies all assumed that there are no defects at the old-new concrete interface. However, there are many microcracks in the interface, which will generate stress concentration at the crack tip, so that the local stress exceeds the ultimate stress strength of the material, leading to the failure of the structure at a low stress level.

Using the theory of concrete fracture mechanics has become a new way to study the development and instability expansion of cracks at the old-new concrete interface [13, 14]. Chen found that adding steel fiber into the new concrete can improve the mode I fracture performance of the old-new concrete interface and increase the sustainability of the post-failure stage [15]. Kurumatani presented an isotropic damage model for concrete based on fracture mechanic [16]. Farnam simulated mode I crack propagation in prestressed concrete sleepers by fracture mechanics [17]. Rezaie investigated the pre-stressed concrete sleepers based on the principles of fracture mechanics in concrete material [18]. Kurumatani developed a method of simulating the cohesive fracture behavior of reinforced concrete while achieving a satisfactory agreement with the experimental results [19].

Scholars have studied the bond mode I fracture performance of old-new concrete, but there are relatively few studies on the bond mode II fracture performance of old-new concrete. However, the crack of concrete structure is often a composite fracture containing both tension and shear effect, especially the fracture between old-new concrete, mainly belongs to mode II fracture [20, 21]. This paper reports the mode II fracture performance of the bonding between old-new concrete. The effects of planting rebar and the basalt fiber are discussed. Nine Z-shaped old-new concrete composite specimens with initial cracks are made. The mode II fracture toughness and fracture energy are adopted as evaluation indexes.

And the regression equations for fracture toughness and fracture energy are deduced with ANOVA.

2. Methods and materials

2.1. Tests design

In this paper, planting rebar number (factor A) and basalt fiber content (factor B) are selected as factors for the mode II fracture performance of old-new concrete. The tests design scheme is given in Table 1.

Table 1. Experimental conditions

Test number		1	2	3	4	5	6	7	8	9
Factors level	A	0	0	0	1	1	1	2	2	2
	B /(kg/m ³)	0	3	6	3	6	0	6	0	3

2.2. Material

(1) Concrete

C40 concrete is adopted. The elastic modulus of C40 concrete is 3.25×10^4 MPa. The compressive strength of C40 concrete is 40 MPa for 150 mm cube. The concrete mix proportion is given in Table 2. The cement is 42.5 grade ordinary Portland cement.

Table 2. Concrete composition /kg

Component	Cement	Water	Sand	Stone
content per m ³	460	195	580	1165

(2) Steel rebar

8HRB400 grade steel rebar is selected. Its diameter is 8 mm, its yield strength is 400 MPa and its ultimate tensile strength is 570 MPa.

(3) Basalt fiber

Basalt fiber is a typical silicate fiber. The average length is 25–30 mm.

2.3. Experimental procedures

2.3.1. Pouring old concrete and planting rebar

The old concrete is L-shaped, as shown in Fig. 1. The artificially surface roughness is 1.67 mm ~ 2.00 mm. At first, use an electric hammer to drill holes. Then, apply brush to the dust of the hole. The diameter of the hole is 10 mm, and the depth is 10 cm. Next,

injecting high-strength anchoring adhesive. At last, insert steel bar or profile, and glue the steel bar and base material into one. The length of planting rebar is 20 cm.

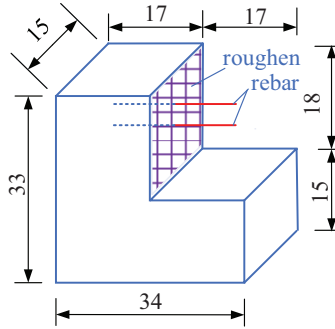


Fig. 1. Old concrete specimen /cm

2.3.2. Pouring new concrete

After 180 days of pouring, the old concrete blocks were soaked in water for 1 day, then the new concrete was poured. In order to study the bonding mode II fracture performance of old-new concrete, specimens were designed as Z-shaped specimen with 30 mm crack [22]. The size of old-new concrete bonding surface is 15×12 cm, as shown in Fig. 2.

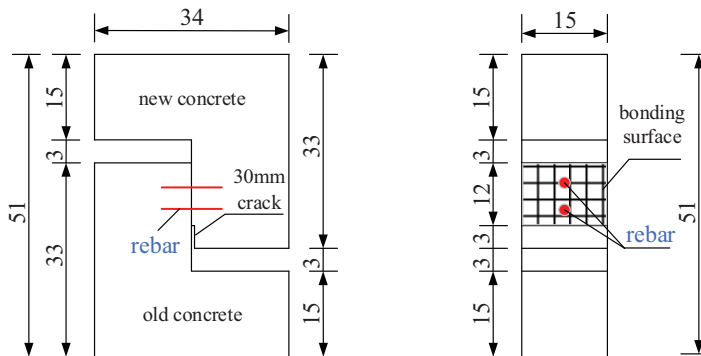


Fig. 2. Z-type specimen /cm

2.3.3. Loading

The hydraulic jack was adopted to load in the test, as shown in Fig. 3. The loading speed was 1 mm/min. The bonding surface was aligned to the center of the jack. There was a steel plate on the loading surface. The force and displacement were measured with press sensor and LVDT in the test.



Fig. 3. Shear test set-up

3. Experimental results

With the loading progress, surface cracks occurred in the old-new concrete interface. The cracks gradually expanded until fracture occurs throughout, coupled with brittle failure sound. When the failure fracture occurred, the old-new concrete specimens were separated along the pouring interface. The aggregate in the section of the new specimen was prominent and the old concrete section was concave. The planting rebar was bending, as shown in Fig. 4.



Fig. 4. Fracture interface

Fig. 5 illustrates the load-displacement relationship curves. The curves are divided according to the planting rebar number in Fig. 5a–5c, and divided according to basalt fiber content in Fig. 5d–5f.

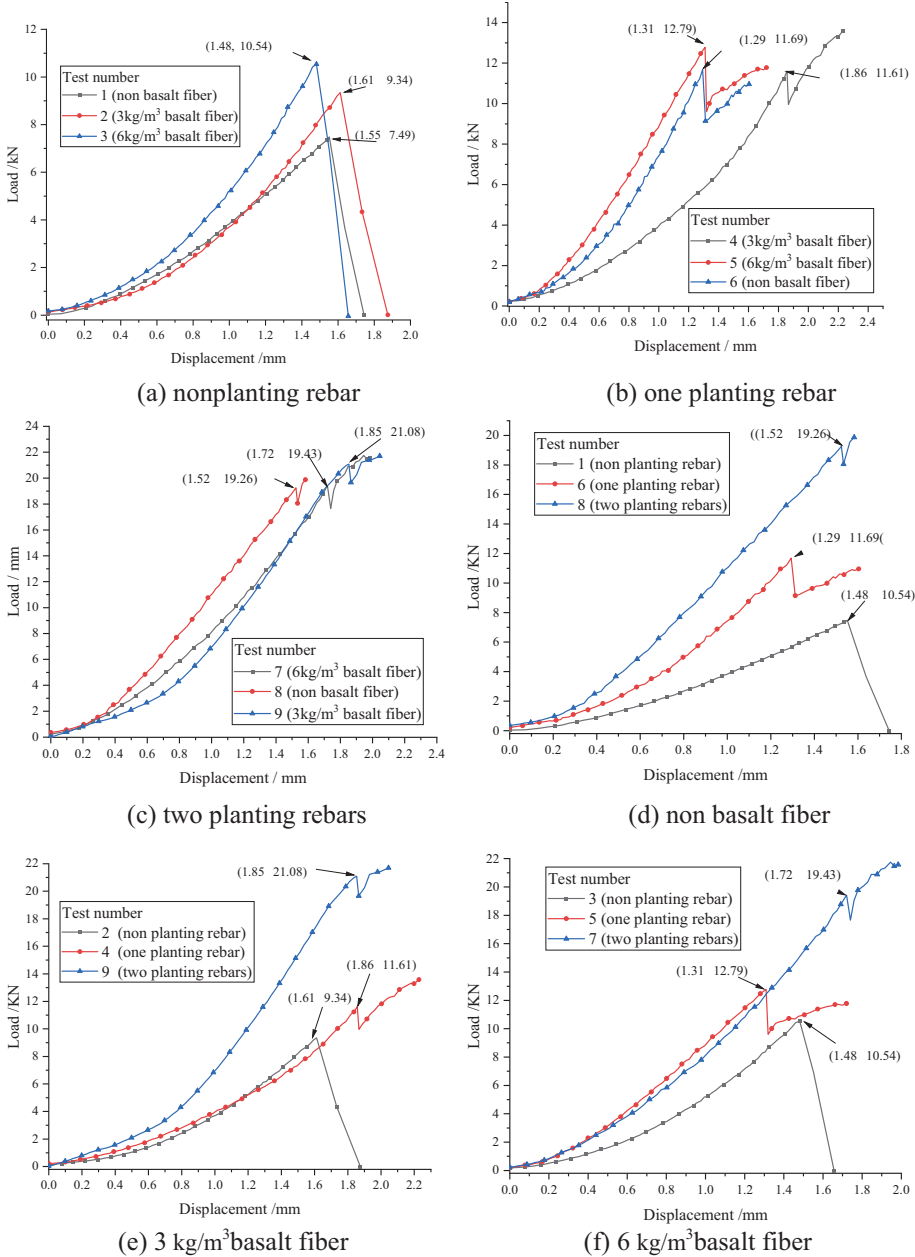


Fig. 5. Load-displacement curve

For the specimen without planting rebar, the load-displacement curves steep descent after the top point. So there appears brittle fracture in the specimen without planting rebar. It can be seen that the maximum failure load and the maximum failure displacement increase with the increase of planting rebar number and basalt fiber content. The maximum failure loads of the specimen without planting rebar, with one planting rebar and with two planting rebars are 10.45 kN, 12.79 kN and 21.08 kN respectively. While the maximum failure displacements of the specimen without planting rebar, with one planting rebar and with two planting rebars are 1.61 mm, 1.86 mm and 1.85 mm. In case of same planting rebar number, the changes of the maximum failure load and the maximum failure displacement are not obvious with the change of basalt fiber content. However, in case of same basalt fiber content, the changes are obvious with the change of planting rebar number. So the shear capacity of old-new concrete increases with the increase of planting rebar number.

4. Discussion

4.1. Mode II fracture performance

4.1.1. Fracture toughness

Irwin proposed K theory, which adopts stress intensity factor to judge the instability and propagation of crack [23]. Mode II fracture toughness is the key stress intensity factor of prefabricated crack under shear load [24, 25]. The pure mode II fracture toughness of Z-shaped specimen can be calculated from Eq. (4.1) [26].

$$(4.1) \quad K_{IIC} = \frac{Q}{BW^{\frac{1}{2}}} f\left(\frac{a}{W}\right)$$

where: Q – fracture load (kN), it can be gotten from Fig. 5; $B = 0.15$ m – specimen thickness (m); $W = 0.15$ m – height of fracture surface of specimen (m); $a = 0.03$ m – notch depth of the crack (m).

$$(4.2) \quad f\left(\frac{a}{W}\right) = \frac{1.945 - 3.547\left(\frac{a}{W}\right) + 3.864\left(\frac{a}{W}\right)^2 - 1.733\left(\frac{a}{W}\right)^3}{\sqrt{1 - \frac{a}{W}}}$$

The mode II fracture toughness of each specimen can be calculated, as shown in Fig. 6a.

4.1.2. Fracture energy

Griffith proposed the G theory, which holds that crack propagation is related to the perspective of fracture energy [27, 28]. The fracture energy is the energy per unit area required for crack propagation under shear load [29, 30], which can be calculated according to Eq. (4.3).

$$(4.3) \quad G_F = \frac{\omega_0 + mg\delta_0}{A_{lig}}$$

where: ω_0 – area under load-displacement curve (N-m), it can be obtained from the test data; $m = 29.376$ kg – new concrete block weight (kg) δ_0 – maximum displacement (m), it can be obtained from Fig. 5; $A_{lig} = \delta_0 \cdot 0.15$ m² – area of broken ligament of concrete (m²). The fracture energy of each specimen can be obtained according to Eq. (4.3), as shown in Fig. 6b.

It can be seen from Fig. 6 that the trends of fracture toughness and fracture energy are almost the same. The fracture toughness and fracture energy increase with the increase of planting rebar number and basalt fiber content. However, the basalt fiber content has little impact on fracture toughness and fracture energy.

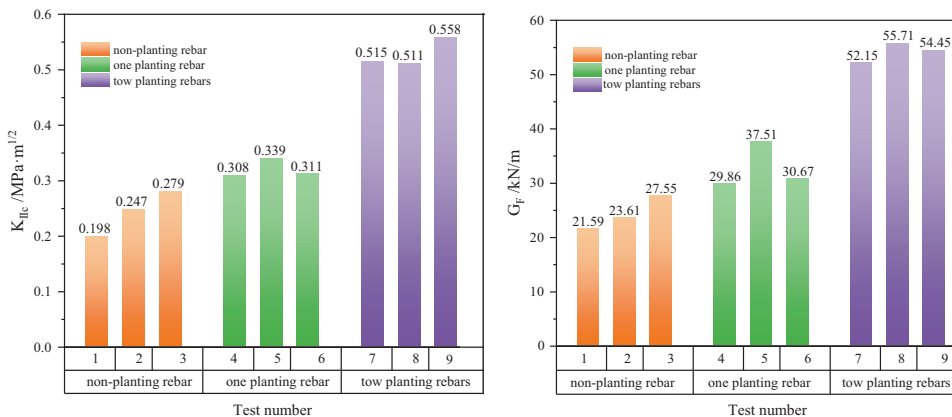


Fig. 6. Fracture performance

4.2. ANOVA

Analysis of variance (ANOVA) was developed by Sir Ronald Fisher to test the significance of the difference between the mean values of two or more samples [31]. If a test result is considered unlikely to occur by chance, given that the null hypothesis is correct, then the result is statistically significant [32]. The regression equations for fracture toughness and fracture energy are deduced as Eq. (4.4), Eq. (4.5). ANOVA for regression equations are presented in Table 3, Table 4.

$$(4.4) \quad y_1 = 7.41 \times 10^{-2} A^2 - 5.03 \times 10^{-4} B^2 - 6.36 \times 10^{-3} AB \\ + 1.38 \times 10^{-2} A + 1.57 \times 10^{-2} B + 2.02 \times 10^{-1}$$

$$(4.5) \quad y_2 = 7.19 A^2 + 0.25 B^2 - 0.78 AB + 2.90 A - 0.23 B + 21.11$$

where: y_1 – fracture toughness, y_2 – fracture energy, A – planting rebar number, B – basalt fiber content.

The P-values of A , B and A^2 are less than 0.0500, which means they are significant model terms for fracture toughness and fracture energy. P-value of B^2 is greater than 0.1000, which indicate B^2 is not significant for fracture toughness and fracture energy.

Table 3. ANOVA for fracture toughness

	Sum of squares	DOF	Mean square	P-value
model	0.1433	5	0.0287	< 0.0001
<i>A</i>	0.1227	1	0.1227	< 0.0001
<i>B</i>	0.0022	1	0.0022	0.0240
<i>A</i> ·	0.0015	1	0.0015	0.0518
<i>A</i> ²	0.0152	1	0.0152	0.0001
<i>B</i> ²	0.0001	1	0.0001	0.6582
residual	0.0019	7	0.0003	
lack of fit	0.0019	3	0.0006	
pure error	0.0000	4	0.0000	
total	.1452	12		

Table 4. ANOVA for fracture energy

	Sum of squares	DOF	Mean square	P-value
model	1598.98	5	319.8	< 0.0001
<i>A</i>	1338.03	1	1338.03	< 0.0001
<i>B</i>	14.11	1	14.11	0.0712
<i>A</i> · <i>B</i>	22.09	1	22.09	0.0325
<i>A</i> ²	142.9	1	142.9	0.0003
<i>B</i> ²	14.52	1	14.52	0.068
residual	21.87	7	3.12	
lack of fit	21.87	3	7.29	
pure error	0	4	0	
total	1620.84	12		

According to Eq. (4.4) and Eq. (4.5), the response surface of planting rebar and basalt fiber content for fracture toughness and fracture energy are gotten, as shown in Fig. 7.

From Fig. 7, it can be seen that planting rebar number is the key factor for mode II fracture performance. With the increase of basalt fiber content, the mode II fracture performance shows a weak improvement. ANOVA verifies the above experimental analysis from the point of mathematical quantitative.

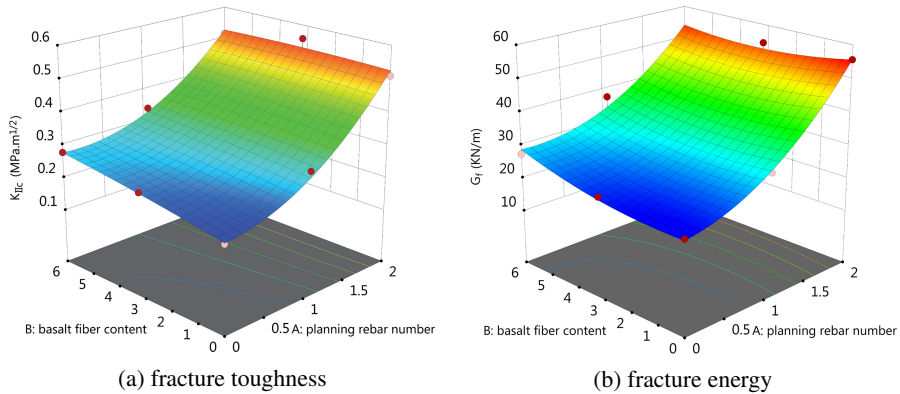


Fig. 7. Response surface plots

5. Conclusions

The mode II fracture properties of the bonding surface of the old-new concrete are experimental studied. And the effects of planting rebar, basalt fiber content are investigated. The conclusions are as follows:

1. The maximum failure load and the maximum failure displacement increase with the increase of planting rebar number and basalt fiber content. The changes of the maximum failure load and the maximum failure displacement are more obvious with the change of planting rebar number. This is because planting rebar could effective improvement the shear capacity of old-new concrete.
2. The fracture toughness and fracture energy increase with the increase of planting rebar number and basalt fiber content. With the increase of the planting rebar number, mode II fracture toughness and fracture energy increase more significantly. So planting rebar is the major factor for mode II fracture performance.

Acknowledgements

This work is supported by the Liaoning Provincial Doctoral Scientific Foundation Projects (20170520138) and the Liaoning Provincial Natural Science Foundation Guidance Projects (2019-ZD-0006).

References

- [1] H.T. Hu, F.M. Lin, H.T. Liu, Y.F. Huang, T.C. Pan, "Constitutive modeling of reinforced concrete and pre-stressed concrete structures strengthened by fiber-reinforced plastics", *Composite Structures*, 2010, vol. 92, no. 7, pp. 1640–1650, DOI: [10.1016/j.compstruct.2009.11.030](https://doi.org/10.1016/j.compstruct.2009.11.030).
- [2] C. Mang, L. Jason, L. Davenne, "A new bond slip model for reinforced concrete structures Validation by modelling a reinforced concrete tie", *Engineering Computations*, 2015, vol. 32, no. 7, pp. 1934–1958, DOI: [10.1108/EC-11-2014-0234](https://doi.org/10.1108/EC-11-2014-0234).

- [3] D. Figueira, A. Ashour, G. Yildirim, A. Aldemir, M. Sahmaran, "Demountable connections of reinforced concrete structures: Review and future developments", *Structures*, 2021, vol. 34, pp. 3028–3039, DOI: [10.1016/j.istruc.2021.09.053](https://doi.org/10.1016/j.istruc.2021.09.053).
- [4] W.W. Wang, J.G. Dai, G. Li, C.K. Huang, "Long-Term Behavior of Prestressed Old-New Concrete Composite Beams", *Journal of Bridge Engineering*, 2011, vol. 16, no. 2, pp. 275–285, DOI: [10.1061/\(ASCE\)BE.1943-5592.0000152](https://doi.org/10.1061/(ASCE)BE.1943-5592.0000152).
- [5] E.K. Tschegg, M. Ingruber, C.H. Surberg, F. Munger, "Factors influencing fracture behavior of old-new concrete bonds", *ACI Materials Journal*, 2000, vol. 97, no. 4, pp. 447–453, DOI: [10.14359/7409](https://doi.org/10.14359/7409).
- [6] J. Jiang, Y.X. Chen, J.W. Dai, "Old-New Concrete Interfacial Bond Slip Monitoring in Anchored Rebar Reinforced Concrete Structure Using PZT Enabled Active Sensing", *Frontiers In Materials*, 2021, vol. 8, DOI: [10.3389/fmats.2021.723684](https://doi.org/10.3389/fmats.2021.723684).
- [7] Y. He, X. Zhang, R.D. Hooton, X. Zhanga, "Effects of interface roughness and interface adhesion on new-to-old concrete bonding", *Construction and Building Materials*, 2017, vol. 151, no. 1, pp. 582–590, DOI: [10.1016/j.conbuildmat.2017.05.049](https://doi.org/10.1016/j.conbuildmat.2017.05.049).
- [8] J. Fan, L. Wu, B. Zhang, "Influence of Old Concrete Age, Interface Roughness and Freeze-Thawing Attack on New-to-Old Concrete Structure", *Materials*, 2021, vol. 14, no. 5, art. ID 1057, DOI: [10.3390/ma14051057](https://doi.org/10.3390/ma14051057).
- [9] W.-W. Wang, J.-g. Dai, G. Li, C.-k. Huang, "Long-Term Behavior of Prestressed Old-New Concrete Composite Beams", *Journal of Bridge Engineering*, 2011, vol. 16, no. 2, pp. 275–285, DOI: [10.1061/\(ASCE\)BE.1943-5592.0000152](https://doi.org/10.1061/(ASCE)BE.1943-5592.0000152).
- [10] C. Maili, M. Jing, "Experimental Study on Shear Behavior of the Interface between New and Old Concrete with Reinforced", *KSCE Journal of Civil Engineering*, 2018, vol. 22, pp. 1882–1888, DOI: [10.1007/s12205-017-2007-6](https://doi.org/10.1007/s12205-017-2007-6).
- [11] X. Zhang, W. Zhang, Y. Luo, L. Wang, "Interface Shear Strength between Self-Compacting Concrete and Carbonated Concrete", *Journal of Materials in Civil Engineering*, 2020, vol. 32, no. 6, DOI: [10.1061/\(ASCE\)MT.1943-5533.0003229](https://doi.org/10.1061/(ASCE)MT.1943-5533.0003229).
- [12] Y. Liang, Z. Lei, L. Dong, C. Bo, "Shear test of the rectangular beam on the new to old concrete interface based on Digital Image Correlation", *IOP Conf. Series: Earth and Environmental Science*, 2019, vol. 267, no. 3, art. ID 032058, DOI: [10.1088/1755-1315/267/3/032058](https://doi.org/10.1088/1755-1315/267/3/032058).
- [13] S.P. Shah, "An overview of the fracture mechanics of concrete", *Cement Concrete and Aggregates*, 1997, vol. 19, no. 2, pp. 79–86, DOI: [10.1520/CCA10319J](https://doi.org/10.1520/CCA10319J).
- [14] K.M.P. Fathima, J.M.C. Kishen, "A thermodynamic correlation between damage and fracture as applied to concrete fatigue", *Engineering Fracture Mechanics*, 2015, vol. 146, pp. 1–20, DOI: [10.1016/j.engfracmech.2015.07.019](https://doi.org/10.1016/j.engfracmech.2015.07.019).
- [15] W. Chen, W. Xie, X. Li, W. Zou, H. Fu, "Determination of fracture energy and fracture toughness of two types of concrete and their interface", *European Journal of Environmental and Civil Engineering*, 2021, vol. 25, no. 1, pp. 104–116, DOI: [10.1080/19648189.2018.1518159](https://doi.org/10.1080/19648189.2018.1518159).
- [16] M. Kurumatani, K. Terada, J. Kato, T. Kyoya, K. Kashiyaama, "An isotropic damage model based on fracture mechanics for concrete", *Engineering Fracture Mechanics*, 2016, vol. 155, pp. 49–66, DOI: [10.1016/j.engfracmech.2016.01.020](https://doi.org/10.1016/j.engfracmech.2016.01.020).
- [17] S.M. Farnam, F. Rezaie, "Simulation of crack propagation in prestressed concrete sleepers by fracture mechanics", *Engineering Failure Analysis*, 2019, vol. 96, pp. 109–117, DOI: [10.1016/j.engfailanal.2018.09.012](https://doi.org/10.1016/j.engfailanal.2018.09.012).
- [18] F. Rezaie, S.M. Farnam, "Fracture mechanics analysis of pre-stressed concrete sleepers via investigating crack initiation length", *Engineering Failure Analysis*, 2015, vol. 58, pp. 267–280, DOI: [10.1016/j.engfailanal.2015.09.007](https://doi.org/10.1016/j.engfailanal.2015.09.007).
- [19] M. Kurumatani, Y. Soma, K. Terada, "Simulations of cohesive fracture behavior of reinforced concrete by a fracture-mechanics-based damage model", *Engineering Fracture Mechanics*, 2019, vol. 206, pp. 392–407, DOI: [10.1016/j.engfracmech.2018.12.006](https://doi.org/10.1016/j.engfracmech.2018.12.006).
- [20] H.W. Reinhardt, S.L. Xu, "A practical testing approach to determine mode II fracture energy G_{IIF} for concrete", *International Journal of Fracture*, 2000, vol. 105, no. 2, pp. 107–125, DOI: [10.1023/A:1007649004465](https://doi.org/10.1023/A:1007649004465).

- [21] Y.W. Chen, J.L. Feng, H. Li, Z.F. Meng, “Effect of coarse aggregate volume fraction on mode II fracture toughness of concrete”, *Engineering Fracture Mechanics*, 2021, vol. 242, DOI: [10.1016/j.engfracmech.2020.107472](https://doi.org/10.1016/j.engfracmech.2020.107472).
- [22] E.N.B.S. Júlio, F.A.B. Branco, V.D. Silva, “Concrete-to-concrete bond strength. Influence of the roughness of the substrate surface”, *Construction and Building Materials*, 2004, vol. 18, no. 9, pp. 675–681, DOI: [10.1016/j.conbuildmat.2004.04.023](https://doi.org/10.1016/j.conbuildmat.2004.04.023).
- [23] G.R. Irwin, “Analysis of Stresses and Strains Near End of a Crack Traversing a Plate”, *Journal of Applied Mechanics*, 1957, vol. 24, pp. 361–364, DOI: [10.1115/1.4011547](https://doi.org/10.1115/1.4011547).
- [24] B. Bahrami, M.R. Ayatollahi, I. Sedighi, M.Y. Yahya, “An insight into mode II fracture toughness testing using SCB specimen”, *Fatigue & Fracture of Engineering Materials & Structures*, 2019, vol. 42, no. 9, pp. 1991–1999, DOI: [10.1111/ffe.13069](https://doi.org/10.1111/ffe.13069).
- [25] M.R. Ayatollahi, M.R.M. Aliha, “On determination of mode II fracture toughness using semi-circular bend specimen”, *International Journal of Solids And Structures*, 2006, vol. 43, no. 17, pp. 5217–5227, DOI: [10.1016/j.ijsolstr.2005.07.049](https://doi.org/10.1016/j.ijsolstr.2005.07.049).
- [26] H. Tada, P.C. Paris, G.R. Irwin, *The stress analysis of cracks handbook*. New York: ASME Press, 2000.
- [27] A.T. Zehnder, “Griffith Theory of Fracture”, in *Encyclopedia of Tribology*, Q.J. Wang, Y.-W. Chung, Eds. Boston, MA: Springer US, 2013, pp. 1570–1573.
- [28] J.-I. Sim, K.-H. Yang, S.-T. Yi, “Effects of Aggregate and Specimen Sizes on Lightweight Concrete Fracture Energy”, *Journal of Materials in Civil Engineering*, 2014, vol. 26, no. 5, pp. 845–854, DOI: [10.1061/\(ASCE\)MT.1943-5533.0000884](https://doi.org/10.1061/(ASCE)MT.1943-5533.0000884).
- [29] S.H.G. Mousavinejad, M.F. Gashti, “Effects of NaOH solution concentration and aging on fracture properties and ductility of ambient-cured heavyweight geopolymer concrete”, *Construction and Building Materials*, 2021, vol. 277, no. 29, art. ID 122266, DOI: [10.1016/j.conbuildmat.2021.122266](https://doi.org/10.1016/j.conbuildmat.2021.122266).
- [30] S. Muralidhara, B.K.R. Prasad, R.K. Singh, “Size independent fracture energy from fracture energy release rate in plain concrete beams”, *Engineering Fracture Mechanics*, 2013, vol. 98, pp. 284–295, DOI: [10.1016/j.engfracmech.2012.10.007](https://doi.org/10.1016/j.engfracmech.2012.10.007).
- [31] M.L. Gaddis, “Statistical methodology: IV. Analysis of variance, analysis of covariance, and multivariate analysis of variance”, *Academic Emergency Medicine*, 1998, vol. 5, no. 3, pp. 258–265, DOI: [10.1111/j.1553-2712.1998.tb02624.x](https://doi.org/10.1111/j.1553-2712.1998.tb02624.x).
- [32] A. Dean, D. Voss, D. Draguljić, *Analysis of Variance and Design of Experiments*. Springer, 2017.

Received: 04.02.2022, Revised: 19.04.2022